

# Value-Gradient based Formulation of Optimal Control Problem and Machine Learning Algorithm

Alain Bensoussan<sup>1,3</sup>, Jiayue Han<sup>3</sup>, Sheung Chi Phillip Yam<sup>4</sup>, and Xiang Zhou<sup>3,5</sup>

<sup>1</sup>Naveen Jindal School of Management, University of Texas at Dallas, Richardson, Texas 75080-3021, U.S.A.

<sup>3</sup>School of Data Science, City University of Hong Kong, Kowloon, Hong Kong SAR

<sup>4</sup>Department of Statistics, Chinese University of Hong Kong, Shatin, N.T., Hong Kong SAR

<sup>5</sup>Department of Mathematics, City University of Hong Kong, Kowloon, Hong Kong SAR

## Abstract

Optimal control problem is typically formulated by Hamilton–Jacobi–Bellman (HJB) equation for the value function and it is well-known that the value function is the viscosity solution of the HJB equation. Once the HJB solution is known, it can be used to construct the optimal control by taking the minimizer of the Hamiltonian. In this work, instead of focusing on the value function, we propose a new formulation for the components of the gradient of the value function (value-gradient) as a decoupled system of partial differential equations in the context of continuous-time deterministic discounted optimal control problem. We develop an efficient iterative scheme for this system of equations in parallel by utilizing the properties that they share the same characteristic curves as the HJB equation for the value function. This property allows us to generalize prior successive approximation algorithms of policy iteration from the value function to the value-gradient functions. To be compatible with the high dimensional control problem, we generate multiple characteristic curves at each policy iteration from an ensemble of initial states, and compute both the value function and its gradient simultaneously on each curve as the labelled data. Then supervised machine learning strategy is applied to minimize the weighted squared loss for both the value function and its gradients. Experimental results of various examples demonstrate that this new strategy of jointly learning both the value function and its gradient not only significantly increases the accuracy but also improves the efficiency and robustness, particularly with less amount of characteristics data or fewer training steps.

## Index Terms

Optimal control, value function, Hamiltonian-Jacobi-Bellman equation, machine learning, characteristic curve.

## I. INTRODUCTION

It is well known that the Hamilton-Jacobi-Bellman(HJB) equation is a central result in optimal control theory for controlling continuous-time differential dynamical systems by the principle of dynamical programming [8], [10], [18], [19]. This equation is a first-order nonlinear partial differential equation (PDE) for the value function which maps an arbitrary given initial state to the optimal value of the cost function. Once this HJB solution is known, it can be used to construct the optimal control by taking the minimizer of the Hamiltonian. Such an optimal control is the feedback control and it does not rely on knowledge of initial conditions. Since the dimension of the HJB equation is the dimension  $d$  of state variable  $x$  in the dynamical system, the size of the state-discretized problems in solving HJB equations increases exponentially with  $d$ . This “curse of dimensionality” has been the long-standing challenge in solving the high dimensional HJB equations, and recently there have been rapid and abundant developments to mitigate this challenge by combining optimal control algorithms with machine learning algorithms, particularly reinforcement learning and deep neural networks [9], [11], [34], [35].

In history, there exists an extensive literature on various numerical methods of finding the approximate solution to the HJB equations. One important idea which attracted a considerable amount of attention is termed the successive approximation method [3]–[5], which aims to handle the nonlinearity in the HJB equation. The successive approximation method reduces the nonlinear HJB equation to an iterative sequence of linear PDEs called the generalized-Hamilton-Jacobi-Bellman (GHJB) equation and the point-wise optimization of taking the minimizer of the Hamiltonian. The GHJB equation is linear since the feedback control is given from the previous iteration. Therefore traditional numerical PDE methods such as Galerkin spectral method (Successive Galerkin approximation [3]) for small  $d$  can be applied to solve these GHJB equations. If the dimension is moderately large, various methods based on low-dimensional representation ansatz such as polynomial or low rank tensor product [20], [23], [31] usually work in many applications. For very high dimensions, the use of deep neural network is prevalent. This two-step procedure in the successive approximation shares exactly the same idea as *policy iteration* in the reinforcement learning [11], [35].

When the Hamiltonian minimization has a closed-form, the HJB equation can be solved directly by using grids and finite difference discretization, such as the Dijkstra-type methods like level method [30], fast marching [38], fast sweeping method [37], and semi-Lagrangian approximation scheme [17]. But these grid-based discretization methods suffer from the curse of dimensionality, i.e., they generally scale exponentially with increases in dimension in the space. There have been tremendous advances in numerical methods and empirical tests now for high dimensional PDEs by taking advantage of neural networks to represent high dimensional functions. For the HJB equation in deterministic optimal control problems, various approaches have been proposed and most of them are based on certain forms of Lagrangian formulation equivalent to the HJB equation. For example, under certain conditions (such as convexity) on the Hamiltonian or the terminal cost, the works in [12]–[15], [27] rely on the generalized Lax and Hopf formulas to transform the computation of the value function at an arbitrary given space-time point as an optimization problem only for the terminal value of the Lagrangian multiplier  $p$ <sup>1</sup>, subject to the characteristics equation of Hamiltonian ODE for  $(x, p)$ . In a similar but different style, [24] worked with the Pontryagin’s maximum principle (PMP) by considering the characteristic equations of the state  $x(t)$  and the co-state  $\lambda(t)$  as a two-point boundary value problem (BVP). The optimal feedback control, the value function and the gradient of the value function on the optimal trajectories are computed first by solving the BVP numerically. With the data generated from the BVP on characteristic trajectories, the HJB solution is then interpolated at any point by either using sparse grid interpolants [25] or minimizing the mean square errors [22], [28], [29]. This step is the standard form of supervised learning, and the numerical accuracy is determined by the quality of the interpolant and the amount of the training data. For a very large  $d$ , the curse of dimensionality is mitigated by the supreme power of deep neural network in deep learning.

In the present paper, we shall develop a new formulation as an alternative to the HJB equation for the optimal control theory and this formulation focuses on the gradient of the value function, instead of the value function itself. For brevity, we call this vector-valued gradient function as *value-gradient* function. One of our motivations is that in practical applications, the optimal feedback control or the optimal policy, is the ultimate goal of the decision maker and this optimal policy is completely determined by the value-gradient in minimizing the Hamiltonian. Another

<sup>1</sup>also called co-state or adjoint variable.

motivation to investigate this value-gradient function comes from the training step where we want to provide the data not only for the value function but also for its gradient to enhance the accuracy of the interpolation. Our new formulation has the following nice properties: (1) It is a closed system of PDEs for components of vector-valued value-gradient functions. (2) This system is essentially decoupled in each component and is perfectly suitable for parallel computation in policy iteration. (3) Each PDE in the system has the exactly same characteristics equation as the original HJB equation for the value function. (4) After simulating characteristics curves, we obtain the results of the value function and the value-gradient function simultaneously on the characteristics curves to train the value function in the whole space.

We demonstrate our innovative method by mainly focusing on the infinite-horizon discounted deterministic optimal control problem. This setup will simplify our presentation since the HJB equation is stationary in time. In addition, we assume the value functions in concern are sufficiently smooth, at least  $C^2$ , which can be guaranteed by imposing appropriate conditions on the state dynamics and the running cost. So, we can interpret the system of PDEs for value-gradient functions in the classic sense. We develop the numerical algorithms based on the *policy iteration* method and the method of characteristics for any arbitrary dimension *per se*. In each policy iteration, only linear equations are solved on the characteristics curves starting from a collection of initial states. The interpolation or the training step is to minimize the convex combination of the mean squared errors of both the value function and the value-gradient functions. The output of our algorithm is still the value function, which is approximated by any type of non-parametric functions like radial basis functions or neural networks. The value-gradient function is obtained by automatic differentiation. Our extensive numerical examples confirm that the accuracy and the robustness are both significantly improved in comparison to solving the HJB equation only with the same policy iteration method. Finally, we remark that a preliminary result in this paper has appeared in the authors' recent manuscript [9] on review of machine learning and control theory. Here we develop the full idea about the value-gradient function formulation and propose the detailed numerical methods in the policy iteration and method of characteristics; in addition, various computational examples of general deterministic control problems are tested here to demonstrate the empirical strength of our new algorithms.

The paper is organized as follows. Section II is the problem setup for the optimal control problem and the review of HJB equations and Pontryagin's maximum principle (PMP) with their connections to optimal control. Section III is our new formulation in terms of the value-gradient

function with some theoretic discussions. Section IV presents our main algorithms and Section V is our numerical examples. Section VI includes some discussions on generalization and ends with a brief conclusion.

## II. PROBLEM FORMULATION AND REVIEW OF HJB EQUATION

### A. Discounted deterministic control problem in infinite horizon

The optimal control problem in our study aims at minimizing the cost function with a discount factor  $\rho \geq 0$ :

$$J_x(u(\cdot)) := \int_0^{+\infty} e^{-\rho t} l(x(t), u(t)) dt \quad (2.1)$$

subject to the state equation

$$\begin{cases} dx(t) = g(x(t), u(t)) dt \\ x(0) = x, \end{cases} \quad (2.2)$$

where  $x(\cdot) : \mathbb{R} \rightarrow \mathbb{R}^d$  is the state variable,  $u(\cdot) : \mathbb{R} \rightarrow \mathbb{R}^p$  is the control function such that  $\int_0^\infty e^{-\rho t} |l(x(t), u(t))| dt < \infty$  and  $u(t) \in \mathcal{U}_{ad}$ , a.e.  $t$ , in which  $\mathcal{U}_{ad}$  is a non-empty closed subset of  $\mathbb{R}^p$ .  $g(\cdot, \cdot) : \mathbb{R}^d \times \mathbb{R}^p \rightarrow \mathbb{R}^d$  and  $l(\cdot, \cdot) : \mathbb{R}^d \times \mathbb{R}^p \rightarrow \mathbb{R}$  have assumptions as below [8]: For some positive constants  $\bar{g}, \bar{l}, \bar{h}, l_0$  and  $c_0$ ,

**A1.**  $g(x, u) : \mathbb{R}^n \times \mathbb{R}^p \rightarrow \mathbb{R}^n$ , is continuously differentiable with bounded and continuously differentiable derivatives  $g_x$  such that

$$|g(x, u)| + |g_x(x, u)| \leq \bar{g} (1 + |x| + |u|); \quad (2.3)$$

**A2.**  $l(x, u) : \mathbb{R}^n \times \mathbb{R}^p \rightarrow \mathbb{R}$ , is continuously differentiable with continuously differentiable derivative  $l_x$  such that

$$\begin{aligned} |l(x, u)| &\leq \bar{l} (1 + |x|^2 + |u|^2); \\ |l_x| + |l_u| &\leq \bar{l} (1 + |x| + |u|); \\ l(x, u) &\geq l_0 |u|^2 - c_0; \end{aligned} \quad (2.4)$$

The value function  $\Phi(x)$  is defined by

$$\Phi(x) = \inf_{u(\cdot) \in \mathcal{U}_{ad}} J_x(u(\cdot)). \quad (2.5)$$

A feedback control  $u$  means there is a function  $a(\cdot)$  in the state variable  $x: \mathbb{R}^d \rightarrow \mathbb{R}^p$ , such that the control  $u(t) = a(x(t))$  with  $x(t)$  satisfying the ODE (2.2) in the autonomous form:  $dx(t) =$

$g(x(t), a(x(t)))dt$ . Throughout the paper, we shall use  $g(x, a)$  and  $g(x, u)$  interchangeably for the function  $g$ . Besides the assumptions above, we assume further that

**A3.** On the optimal trajectory  $x^*(\cdot)$ , the value function and its gradient satisfy  $\lim_{t \rightarrow \infty} e^{-\rho t} \Phi(x^*(t)) = 0$  and  $\lim_{t \rightarrow \infty} e^{-\rho t} \nabla \Phi(x^*(t)) = 0$ . This assumption can be satisfied for example, if  $\Phi$  at most has the polynomial growth [19].

**Notations:**  $\nabla$  and  $\nabla^2$  refer to the gradient and Hessian matrix, respectively, of a scalar function.  $D$  is used for the derivatives of a vector-valued function, i.e., the Jacobian matrix. For example,  $D_x g(x, a)$  refers to the Jacobi matrix in  $x$  variable with  $(i, j)$  entry  $\frac{\partial g_i}{\partial x_j}(x, a)$ .  $D_x^\top g$  means the transpose of the Jacobi matrix  $D_x g$ .

### B. Hamiltonian-Jacobi-Bellman equation

By the theory of Dynamic Programming, the value function  $\Phi(\cdot)$  of (2.5) satisfies the (stationary) Hamilton-Jacobi-Bellman (HJB) equation

$$\rho \Phi(x) = \min_a [g(x, a) \cdot \nabla \Phi(x) + l(x, a)] \quad (2.6)$$

which can be split into the coupled system of both value and policy functions

$$\rho \Phi(x) = g(x, \hat{a}(x)) \cdot \nabla \Phi(x) + l(x, \hat{a}(x)), \quad (2.7)$$

where the optimal policy is

$$\hat{a}(x) \in \operatorname{argmin}_a [g(x, a) \cdot \nabla \Phi(x) + l(x, a)]. \quad (2.8)$$

We drop out the possible constraint  $a \in \mathcal{U}_{ad}$  under  $\operatorname{argmin}$  or  $\min$  for convenience. The first equation (2.7) is a *linear* stationary hyperbolic PDE with advection velocity field  $g(x, \hat{a}(x))$ .

It is the convention to introduce the Hamiltonian

$$H(x, \lambda, a) := g(x, a) \cdot \lambda + l(x, a)$$

and the minimized Hamiltonian

$$\mathbb{H}(x, \lambda) = \min_a H(x, \lambda, a). \quad (2.9)$$

The HJB equation (2.6) can be written as

$$\rho \Phi(x) = \mathbb{H}(x, \nabla \Phi(x)).$$

**Remark 1.** The minimization subproblem (2.8) can have the analytical solution in certain cases including the linear-quadratic regulator. To be specific, if  $g(x, a) = A(x) + Ba$  and  $l(x, a) = L(x) + \frac{1}{2}a^\top Na$  with two matrices  $B$  and  $N$ , then we have  $\hat{a}(x) = -N^{-1}B^\top \nabla \Phi(x)$ .

### C. Pontryagin's maximum principle (PMP)

Pontryagin's maximum principle generally refers to the first-order necessary optimality conditions for problems of optimal control [32]. For the optimal control problem specified in Section II-A, the PMP takes the following form

$$\frac{d}{dt}x^*(t) = H_\lambda(x^*, \lambda^*, u^*) = g(x^*, u^*) \quad (2.10a)$$

$$\begin{aligned} \frac{d}{dt}e^{-\rho t}\lambda^*(t) &= -e^{-\rho t}H_x(x^*, \lambda^*, u^*) \\ &= -e^{-\rho t}[\nabla_x l(x^*, u^*) + D_x^\top g(x^*, u^*)\lambda^*] \end{aligned} \quad (2.10b)$$

$$\frac{d}{dt}e^{-\rho t}v^*(t) = -e^{-\rho t}l(x^*, u^*) \quad (2.10c)$$

where  $u^*(t) \in \mathcal{U}_{ad}$  is defined by  $\hat{a}(x^*(t))$  in (2.8), i.e.,  $u^*(t) = \underset{u}{\operatorname{argmin}} H(x^*(t), u, \lambda^*(t))$ .  $\lambda^*(t)$  is the co-state or adjoint variable and  $v^*$  is the cost. Note that (2.10a) has the initial condition  $x^*(0) = x$  while (2.10b) and (2.10c) have the terminal condition vanishing at infinity:  $e^{-\rho t}\lambda^*(t) \rightarrow 0$  and  $e^{-\rho t}v^*(t) \rightarrow 0$  with the assumption A3. Along the optimal trajectory  $x^*(t)$ , we have that the value function and its gradient are  $\Phi(x^*(t)) = v^*(x^*(t))$  and  $\nabla\Phi(x^*(t)) = \lambda^*(t)$ , respectively and the optimal feedback control is  $\hat{a}(x^*(t)) = u^*(t)$ .

### D. Value iteration and policy iteration for HJB equation

By regarding the equations (2.7) and (2.8) as a fixed-point problem for the pair of  $\Phi$  and  $\hat{a}$ , many iterative computational methods have been developed in history [6], [7], [21]. They can roughly be divided into two categories: value iteration and policy iteration, which are central concepts in reinforcement learning [35].

In our model of equation (2.6), the value iteration, roughly speaking, refers to the sequence of functions recursively defined by

$$\Phi^{k+1}(x) := \rho^{-1} \min_a [g(x, a) \cdot \nabla\Phi^k(x) + l(x, a)], \quad \forall x. \quad (2.11)$$

The policy iteration requires to solve the Generalized HJB equation. It starts with an initial policy function  $a^0$  and runs the iteration from  $a^k$  to  $a^{k+1}$  as follows.

**Algorithm 1** (Policy Iteration (Successive Approximation) for HJB equation).

- 1) Firstly, solve the linear PDE (2.7) for the value function  $\Phi^{k+1}$  with the given policy  $\hat{a} = a^k$ :

$$\rho\Phi^{k+1}(x) = g(x, a^k(x)) \cdot \nabla\Phi^{k+1}(x) + l(x, a^k(x)). \quad (2.12)$$

This equation is referred to as Generalized HJB equation.

2) Then,  $a^{k+1}$  is obtained from the optimization sub-problem (2.8) point-wisely for each  $x$ :

$$a^{k+1}(x) := \underset{a}{\operatorname{argmin}} [g(x, a) \cdot \nabla \Phi^{k+1}(x) + l(x, a)].$$

Step 1) is usually referred to as *policy evaluation*. Step 2) is usually referred to as *policy improvement* and  $a^{k+1}$  is the *greedy policy*.

The policy iteration is known to have super-linear convergence in many cases provided the initial guess is sufficiently close to the solution and generally behaves better than the value iteration [1]. The convergence of policy iteration can be found in [33], which treated the policy iteration as Newton-Kantorovich iteration procedure applied to the functional equation of dynamic programming.

**Example 1 (LQR).** As an example, we write the policy iteration for the linear-quadratic regulator (LQR) problem. Linear quadratic case is a special case of optimal control problem where  $g(x, a) = Ax + Ba$  and  $l(x, a) = \frac{1}{2}x^\top Mx + \frac{1}{2}a^\top Na$  with  $M$  and  $N$  positive definite. Then the value function takes the quadratic form  $\Phi(x) = \frac{1}{2}x^\top Px$  with the symmetric  $P$  to be determined. Write  $\Phi^k = \frac{1}{2}x^\top P^k x$  with a symmetric initial  $P^0$ . The control law is then given by (2.8):  $a^k(x) = -N^{-1}B^\top P^k x$ . The value iteration of (2.11) now becomes

$$P^{k+1} = \frac{1}{\rho} \left[ A^\top P^k + (P^k)^\top A - (P^k)^\top B(N^{-1})B^\top P^k + M \right]$$

The policy iteration (2.12) is to solve the matrix-equation

$$\begin{aligned} \rho P^{k+1} &= P^{k+1}A + A^\top P^{k+1} - 2P^k B N^{-1} B^\top P^{k+1} \\ &\quad + M + P^k B N^{-1} B^\top P^k \end{aligned} \tag{2.13}$$

These are two iterative schemes for the algebraic Riccati equation for the true  $P$ :

$$\rho P = PA + A^\top P + M - PBN^{-1}B^\top P. \tag{2.14}$$

### III. FORMULATION FOR VALUE-GRADIENT FUNCTIONS

We start to present our main theoretic results and derive the new system of PDEs for the gradient of the value function.



### A. Equation for the value-gradient functions

Define the *value-gradient* function:

$$\lambda(x) = \nabla\Phi(x),$$

then the HJB equation (2.7) reads

$$\rho\Phi(x) = g(x, \hat{a}(x)) \cdot \lambda(x) + l(x, \hat{a}(x)). \quad (3.15)$$

where  $x = (x_1, \dots, x_d) \in \mathbb{R}^d$ . Now differentiating both sides w.r.t.  $x_i$ , we have

$$\begin{aligned} \rho\lambda_i(x) &= \sum_n \lambda_n(x) \left\{ \left( \frac{\partial}{\partial x_i} + \sum_j \frac{\partial \hat{a}_j}{\partial x_i} \frac{\partial}{\partial a_j} \right) g_n(x, \hat{a}(x)) \right\} \\ &+ \sum_n g_n(x, \hat{a}(x)) \frac{\partial \lambda_n}{\partial x_i}(x) + \left( \frac{\partial}{\partial x_i} + \sum_j \frac{\partial \hat{a}_j}{\partial x_i} \frac{\partial}{\partial a_j} \right) l(x, \hat{a}(x)). \end{aligned}$$

We assume that the Hamiltonian minimization (2.8) has the unique minimizer  $\hat{a}(x)$  which is continuously differential. Then the minimizer  $\hat{a}(x)$  satisfies the first order necessary condition:

$$\sum_n \frac{\partial g_n}{\partial a_j}(x, \hat{a}) \lambda_n(x) + \frac{\partial l}{\partial a_j}(x, \hat{a}) = 0, \quad \forall j. \quad (3.16)$$

With the both equalities above, we have that  $\lambda(x) = (\lambda_1, \dots, \lambda_d)$  satisfies the following system of linear hyperbolic PDEs

$$\rho\lambda_i = \sum_n g_n \frac{\partial \lambda_n}{\partial x_i} + \sum_n \lambda_n \frac{\partial g_n}{\partial x_i} + \frac{\partial l}{\partial x_i}, \quad (3.17)$$

or in the compact form

$$\begin{aligned} \rho\lambda(x) &= D^\top \lambda(x) g(x, \hat{a}(x)) + D_x^\top g(x, \hat{a}(x)) \lambda(x) \\ &+ \nabla_x l(x, \hat{a}(x)), \end{aligned} \quad (3.18)$$

and  $\hat{a}(x)$  defined by (2.8) can now be written as

$$\hat{a}(x) \in \operatorname{argmin}_a [g(x, a) \cdot \lambda(x) + l(x, a)]. \quad (3.19)$$

(3.18) and (3.19) are coupled as (2.7) and (2.8) in the HJB equation and they serve as the foundation for the new development of the algorithms, based on the policy iteration method.

Given a policy  $\hat{a}$ , the system of coupled PDEs (3.18) is a closed form involving only the dynamic function  $g$  and the running cost function  $l$ ; it does not need other information like the value function. It plays the similar role to the Generalized HJB equation (2.7) for the value function  $\Phi$ . (3.18) and (3.19) together can replace the traditional dynamic programming in the

form of HJB equation (2.6) if  $\Phi$  is sufficiently smooth. The main focus of our work is how to develop efficient numerical methods from this formulation of the gradient of the value function.

We have the proposition below to write the system (3.18) more friendly. Since  $\lambda(x)$  is the gradient of the value function  $\Phi$ , so  $D\lambda(x) = \nabla^2\Phi(x)$  should be symmetric, i.e.,  $D\lambda = D^\top\lambda$ . However, we do not know this symmetry *a priori* and indeed we can verify  $\frac{\partial\lambda_i}{\partial x_j} = \frac{\partial\lambda_j}{\partial x_i}$  based on equation (3.17) only.

**Proposition 1.** *If  $\lambda$  satisfies (3.18) (i.e. (3.17)), then*

$$D\lambda = D^\top\lambda, \quad \text{i.e.}, \quad \frac{\partial\lambda_i}{\partial x_j} = \frac{\partial\lambda_j}{\partial x_i}, \forall i, j.$$

*Proof.* Taking derivative for (3.17) w.r.t.  $x_j$  and a direct calculation immediately shows the conclusion by noting the Hessian of  $l$  is symmetric:  $\frac{\partial^2 l}{\partial x_i \partial x_j} = \frac{\partial^2 l}{\partial x_j \partial x_i}$ .  $\square$

**Theorem 2.** *Suppose  $\Phi$  is the solution of the HJB equation satisfying the assumption A1,A2,A3, then the value-gradient  $\nabla\Phi$  satisfies*

$$\rho\lambda_i(x) = \nabla\lambda_i(x) \cdot g(x, \hat{a}(x)) + \sum_n \frac{\partial g_n}{\partial x_i} \lambda_n(x) + \frac{\partial l}{\partial x_i}(x, \hat{a}(x)) \quad (3.20)$$

or

$$\rho\lambda(x) = (D\lambda)g + (D_x^\top g)\lambda(x) + \nabla_x l. \quad (3.21)$$

where  $\hat{a}(x)$  is defined in (3.19) as the unique minimizer of the Hamiltonian  $H(x, \lambda(x))$ . In addition, if  $\lambda(x)$  satisfies the systems of PDEs (3.20), then for  $x^*$  as the optimal trajectory satisfying the characteristics equation (2.10a), then  $\lambda^*(t) := \lambda(x^*(t))$  satisfies the equation (2.10b).

The conclusion that  $\lambda^*(t) := \lambda(x^*(t))$  satisfies (2.10b) follows from the following fact

$$\frac{d}{dt}\lambda(t) = (\nabla\lambda)g = \rho\lambda^*(t) - [(D_x^\top g)\lambda(x) + \nabla_x l].$$

The advantage of equation (3.20) over the equation (3.17) is that the advection terms  $\nabla\lambda_i \cdot g$  are now decoupled for each component  $i$  and the same as in the GHJB (2.7). This property will allow us to develop a fully paralleled iterative method.

### B. Policy iteration for $\lambda$

The natural idea to solve the PDEs for (3.20) and the minimization for  $\hat{a}$  in (3.19) is the policy iteration by recursively solving (3.20) and (3.19) like the policy iteration for the value function dictated in Section II-D: Start with an initial policy function  $a^0$  with  $k = 0$ ;

- 1) Solve the system (3.20) with the given policy  $\hat{a} = a^k$  to have  $\lambda^{k+1}$ ;
- 2)  $a^{k+1}$  is obtained from the optimization sub-problem (2.8):

$$a^{k+1}(x) = \underset{a}{\operatorname{argmin}} [g(x, a) \cdot \lambda^{k+1}(x) + l(x, a)].$$

This iteration will produce a sequence of pairs  $(a^k, \lambda^k)$ ,  $k \geq 1$ . The main task is then to solve (3.20) (or (3.21)), the system of linear PDEs for  $\lambda(x)$ , with a given policy  $a$ . We will propose the method for this system of linear PDEs below and more details are given in Section IV.

For convenience, we introduce a mapping  $\mathcal{T}_a$  associated with a given control law  $a(x)$ :

$$\lambda(\cdot) \rightarrow \Lambda(\cdot) := \mathcal{T}_a \lambda(\cdot)$$

with  $\Lambda(\cdot)$  defined as the solution to the PDE system for any arbitrary input  $\lambda(\cdot)$

$$\rho \Lambda(x) - (D\Lambda)g = (D_x^\top g)\lambda(x) + \nabla_x l. \quad (3.22)$$

where  $g = g(x, a(x))$  and  $l = l(x, a(x))$ . Then the solution to (3.21) is the fixed point of the mapping  $\mathcal{T}_{a^k}$ . We formulate the following recursive scheme for (3.20) in this single policy iteration, starting with  $\lambda^{k+1,0} = \lambda^k$  and for  $m = 0, 1, \dots$ ,

$$\begin{aligned} & \rho \lambda_i^{k+1,m+1}(x) - \nabla \lambda_i^{k+1,m+1}(x) \cdot g(x, a^k(x)) \\ &= \sum_n \frac{\partial g_n}{\partial x_i} \lambda_n^{k+1,m}(x) + \frac{\partial l}{\partial x_i}(x, a^k(x)). \end{aligned} \quad (3.23)$$

Here, the  $i$ -th component of  $\lambda$  is denoted by the subindex  $i$ .  $k$  is fixed in this inner loop of  $m$ . The recursive scheme (3.23) is a fixed-point iteration of the equation (3.20):  $\lambda^{k+1,m} = (\mathcal{T}_{a^k})^m \lambda^k$  and is expected to converge to the true solution  $\lambda^{k+1}$  as  $m$  tends to infinity. In principle, this inner loop of  $m$  should be computed with sufficiently  $M$  steps and  $\lambda^{k+1,M}$  is the numerical approximation of  $\lambda^{k+1}$ . However, setting  $M = 1$  for the inner loop practically works efficiently by letting

$$\lambda^{k+1} = \mathcal{T}_{a^k} \lambda^k \quad (3.24)$$

So we have the following **PI-lambda** algorithm.

**Definition 1 (PI-lambda:** policy iteration based on  $\lambda$  ).

Start with an initial policy function  $a^0$  with  $k = 0$ ;

1) For  $i = 1, \dots, d$ , solve the PDE for each  $\lambda_i^{k+1}$  in parallel

$$\begin{aligned} & \rho \lambda_i^{k+1}(x) - \nabla \lambda_i^{k+1}(x) \cdot g(x, a^k(x)) \\ &= \sum_n \frac{\partial g_n}{\partial x_i} \lambda_n^k(x) + \frac{\partial l}{\partial x_i}(x, a^k(x)), \end{aligned} \quad (3.25)$$

with the given policy  $\hat{a} = a^k$  to have  $\lambda^{k+1} = (\lambda_1^{k+1}, \dots, \lambda_d^{k+1})$ ;

2)  $a^{k+1}$  is obtained from the optimization sub-problem (2.8):

$$a^{k+1}(x) = \underset{a}{\operatorname{argmin}} [g(x, a) \cdot \lambda^{k+1}(x) + l(x, a)].$$

The merit of (3.25) is that the components of  $\lambda^{k+1}(x)$  are completely decoupled and can be solved in parallel. Each equation of these  $d$  components is exactly in the same form as the GHJB equation (2.12) for the value function. So the method of characteristics, which will be detailed in the next section, can be applied to both the GHJB equation (2.12) and the system (3.25).

Before we march to the numerical methods, we discuss the case of linear-quadratic regulator.

**Example 2 (LQR (continued)).** For the LQR in Example 1, we have  $\lambda(x) = \nabla \Phi(x) = Px$  and the equation for  $\lambda$  (3.21) is just the same Riccati equation (2.14). But in **PI-lambda**, (3.25) with  $\lambda^{k+1}(x) = P^{k+1}x$  leads to a new iterative scheme

$$\rho P^{k+1} - P^{k+1}(A - BN^{-1}B^T P^k) = M + A^T P^k \quad (3.26)$$

or equivalently,

$$P^{k+1} = (M + A^T P^k)(\rho I - A + BN^{-1}B^T P^k)^{-1}$$

which is different from (2.13) and in fact it is easier to solve than (2.13).

### C. Convergence Analysis

[9] considers a generalization of the LQR case, where

$$g(x, a) = A(x) + Ba, \quad \text{and} \quad l(x, a) = L(x) + \frac{1}{2}a^T Na. \quad (3.27)$$

Under some mild conditions for the function  $A(x)$  and  $L(x)$ , when  $\rho$  is sufficiently large, the system of PDE (3.20) has the unique solution  $\lambda$  with  $\lambda$  and  $D\lambda$  both bounded. So, our assumption **A3** is satisfied. And the policy iteration based on lambda converges if the initial  $\lambda^0$  and  $D\lambda^0$  are

sufficiently small. The details can be founded in [9] and we shall not elaborate these theoretical analysis in this paper and the remaining sections are mainly devoted to the design of practical numerical methods for high dimensional setting.

#### IV. NUMERICAL METHODS

Our algorithm is the policy iteration based on  $\lambda$  and it is clear that the main challenge is to solve the system of linear PDEs (3.25) in any dimension. It is worthwhile to point out that each PDE in (3.25) is the same type of PDE as the GHJB (2.12). So, the Galerkin approximate approach can be also applied for these equations in (3.25), but to directly aim for the high dimensional problems, we use the method of characteristics and the supervised learning.

Specifically, we first consider a family of functions, such as neural networks,  $\widehat{\Phi}(x; \theta)$  to numerically represent the value function, where  $\theta \in \Theta$  is the set of parameters. The gradient-value function  $\widehat{\lambda}(x; \theta) = \nabla_x \widehat{\Phi}(x; \theta)$  is then computed by automatic differentiation instead of finite difference. Secondly, in each policy iteration  $k$ , we compute the characteristics by numerical integrating the state dynamics and calculate the true value  $\Phi^{k+1}$  and gradient-value functions  $\lambda^{k+1}$  on the characteristics curves based on the PDE (2.12) and (3.25). Then these labelled data  $(X(t), \Phi(X(t)), \lambda(X(t)))$  are fed into the supervised learning protocol by minimizing the mean squared errors. to find the optimal  $\theta^{k+1}$ . The main idea is illustrated in Figure 1.

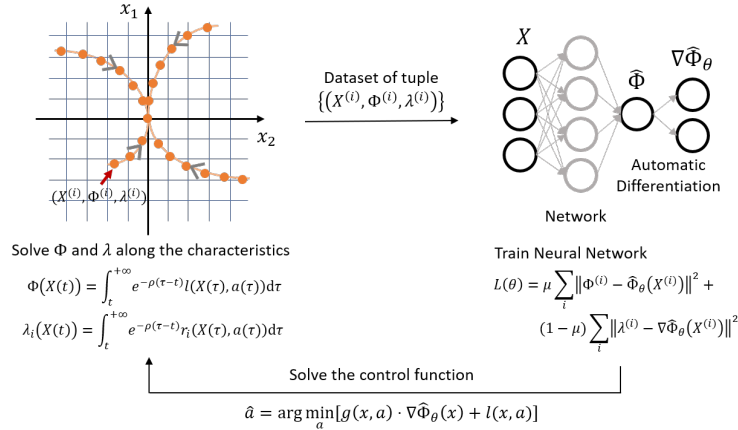


Fig. 1: Illustration of the **PI-lambda** algorithm

In sequel, we discuss the details of method of characteristics on solving the PDEs (2.12) and (3.25) on characteristics curves. We drop the **PI-lambda** iteration index  $k$  in this section to

notational ease.

### A. Method of characteristics

Bearing in mind the similar form of (2.12) and (3.25) which are both hyperbolic linear PDEs with the same advection, we consider a general discussion. Given a control function  $a(\cdot)$ , we denote

$$G(x) = g(x, a(x))$$

and define  $X(t)$  as the characteristic curve satisfying the following ODE with an arbitrary initial state  $X_0 \in \mathbb{R}^d$ :

$$\begin{cases} dX(t) = G(X)dt, \\ X(0) = X_0. \end{cases} \quad (4.28)$$

We consider the following PDE of the function  $u$

$$\rho u(x) - \nabla u(x) \cdot G(x) = R(x) \quad (4.29)$$

where the source term  $R$  is given. Note that (2.12) and (3.25) are special cases of (4.29) with different  $R$  terms.

Along the characteristic curve  $X(t)$ , by (4.28) and (4.29) we derive that

$$\begin{aligned} & \frac{d}{dt} [e^{-\rho t} u(X(t))] \\ &= -\rho e^{-\rho t} u(X(t)) + e^{-\rho t} \nabla u(X(t)) \cdot G(X(t)) \\ &= -e^{-\rho t} R(X(t)). \end{aligned}$$

After taking integral in time,

$$e^{-\rho t} u(X(t)) - u(X_0) = \int_0^t -e^{-\rho \tau} R(X(\tau)) d\tau \quad (4.30)$$

As time  $t$  tends to infinity,

$$u(X_0) = \lim_{t \rightarrow +\infty} e^{-\rho t} u(X(t)) + \int_0^{+\infty} e^{-\rho \tau} R(X(\tau)) d\tau.$$

If  $\lim_{t \rightarrow +\infty} e^{-\rho t} u(X(t)) = 0$ , then  $u(X_0) = \int_0^{+\infty} e^{-\rho \tau} R(X(\tau)) d\tau$  and for any  $t \geq 0$ ,

$$u(X(t)) = \int_t^{+\infty} e^{-\rho(\tau-t)} R(X(\tau)) d\tau. \quad (4.31)$$

**Remark 2.** If  $\rho = 0$ , we only have  $u(X(t)) - u(X_0) = \int_0^t R(X(s)) ds$ . In this case, to determine the value  $u(X(t))$  for any  $t$ , the value  $u(X_0)$  at the initial  $X_0$  is necessary, which could be approximated by bootstrap idea like using  $u^k(X_0)$  from the prior policy iteration.

### B. Compute the value function and the gradient on the characteristics

We apply the above method of characteristics to compute the value function  $\Phi$  and the gradient  $\lambda = \nabla\Phi$ . For the value function in equation (2.7), the  $R$  function in (4.29) is  $l(x, a(x))$ . Then  $\Phi$  in (2.7) has the values on  $X(t)$ :

$$\Phi(X(t)) = \int_t^{+\infty} e^{-\rho(\tau-t)} l(X(\tau), a(X(\tau))) d\tau. \quad (4.32)$$

For  $\lambda^{k+1}$  in (3.25), for each component  $i$ ,  $R(x)$  in (4.29) now refers to the right hand side in function (3.25), then

$$\lambda_i^{k+1}(x(t)) = \int_t^{+\infty} e^{-\rho(\tau-t)} r_i(\tau) d\tau. \quad (4.33)$$

where  $r_i(\tau) = \sum_n \frac{\partial g_n}{\partial x_i} \lambda_n^k(X(\tau)) + \frac{\partial l}{\partial x_i}(X(\tau), a^k(X(\tau)))$ .

### C. Supervised learning: interpolate the characteristic curve to the whole space

With a characteristic curve  $X(\cdot)$  computed from (4.28), we can obtain the value of the value function  $\Phi$  and the gradient  $\lambda_i = \frac{\partial\Phi}{\partial x_i}$ ,  $i = 1, \dots, d$ , along  $X(t)$  *simultaneously*. By running multiple characteristic curves starting from a set of the initial points  $\{X_0^{(n)}, 1 \leq n \leq N\}$  which are generally sampled uniformly, we obtain a collection of observations of  $\Phi(X^{(n)}(t))$  and  $\lambda(X^{(n)}(t))$  on these characteristics trajectories  $\{X^{(n)}(t) : t \geq 0, 1 \leq n \leq N\}$ . In practice, the continuous path  $X^{(n)}(t)$  is represented by a finite number of ‘‘images’’ on the curve and these images on each curve are chosen to have the roughly equal distance to each neighbouring image.

To interpolate the labelled data from the computed curves to the whole space, a family of approximate functions  $\widehat{\Phi}(x; \theta)$  should be proposed first by the users, which could be Galerkin form of basis functions or radial basis function or neural networks with certain architectures, etc. Then the parameters  $\theta$  is found by minimizing the following loss function  $L(\theta)$  combining two mean square errors:

$$\begin{aligned} L(\theta) &= \mu \sum_{n=1}^N \int \left| \Phi(X^{(n)}(t)) - \widehat{\Phi}_\theta(X^{(n)}(t)) \right|^2 dt \\ &+ (1 - \mu) \sum_{n=1}^N \int \left\| \lambda(X^{(n)}(t)) - \nabla \widehat{\Phi}_\theta(X^{(n)}(t)) \right\|^2 dt \end{aligned} \quad (4.34)$$

where  $0 \leq \mu \leq 1$  is a factor to balance the loss from the value function and the gradient.  $\|\cdot\|$  is the Euclidean norm in  $\mathbb{R}^d$ . The gradient  $\nabla \widehat{\Phi}$  is the gradient w.r.t. the state variable  $x$  and computed by automatic differentiation. The training process of the models is to minimize the

loss function (4.34) w.r.t.  $\theta$  by some standard gradient-descent optimization methods such as ADAM [26].

A few remarks are discussed now to explain our practical algorithm more clearly.

- Our algorithmic framework is the policy iteration based on  $\lambda$ . So the computation of the data points on the characteristics curves and the training of the loss (4.34) are performed at each policy iteration  $k$ . One can adjust the number of characteristic trajectories  $N$  and the number of training steps (the steps within the minimization procedure for the loss function). The trajectory number  $N$  determines the amount of data and the training step determines the computational time in training. For efficiency issue, these two numbers can be adaptively tuned practically to balance the tradeoff between the computational burden in each policy iteration and the total number of policy iterations.
- The loss (4.34) simply writes the contribution from each trajectory in the continuous  $L_2$  integration in time. Practically, this integration is represented by the sum from each discrete points on the curves. For better fitting the function  $\widehat{\Phi}_\theta$ , in contrast to the ODE solver used to solve the the characteristics ODEs, these points are not supposed to correspond to equal step size in time variable, but these points should be selected or arranged to spread out evenly in space when all trajectories are considered. There are many practical ways to achieve this target such as using the arc-length parametrization or setting a small ball as the forbidden region for each prior points. Our numerical tests use the arc-length parametrization for each trajectory.
- The choice of the initial states  $\{X_0^{(n)} : 1 \leq n \leq N\}$  can affect how the corresponding characteristics curves behave in the space and we hope these finite number of curves can *explore* the space efficiently. Some adaptive ideas are worth a try in practice too. For example, more points may be sampled where the residual of HJB equation is larger. However, since the whole characteristics curves nonlinearly depends on the initial, we use the uniform distribution in our numerical tests for simplicity. These initial states can be the same for all policy iterations or be sampled again after each policy iteration.

## V. NUMERICAL EXAMPLES

This section presents the numerical experiments on three examples to show the advantage of our new method of the policy iteration using  $\lambda$  and  $\Phi$  over the method only using  $\Phi$ . The three problems we tested are the following:



- Linear-quadratic regulator.
- Pendulum swing-up task.
- Cart-pole balancing task.

### A. Linear Quadratic Problem

The control problem to be solved is a  $d$ -dim linear-quadratic case with the cost function

$$J(u) = \int_0^{\infty} e^{-\rho t} (\|x\|^2 + \|u\|^2) dt$$

subject to the dynamic system

$$\frac{dx}{dt} = Ax + Bu, \quad x(0) = x_0.$$

Instead of solving the Riccati equation for this problem, we apply our method in Section IV by using the network structure

$$\hat{\Phi}_Q(x) = \frac{1}{2} x^\top (Q^\top + Q)x$$

for simplicity where  $Q$  is the parameter to be determined, since we know the true value function is a quadratic function. This type of parametrization can eliminate the approximation error since the true value function belong to this family of parametrized functions.

We apply the algorithm to the following three choices of  $A$  with  $d = 5$ ,  $B = I_d$  and  $\rho = 1$ .

- Test 1:  $A = I_d$  where  $I_d$  is the  $d$ -dim identical matrix.
- Test 2 :  $A = (a^T a + I_d)/d$  where  $a$  is an  $d$ -by- $d$  matrix. Every component of  $a$  is i.i.d. random variables sampled from standard normal distribution. The generated  $A$  is

$$A = \begin{bmatrix} 0.819 & 0.173 & 0.828 & 0.318 & -0.354 \\ 0.173 & 0.816 & 0.318 & 0.178 & -0.205 \\ 0.828 & 0.318 & 1.717 & 0.622 & -0.175 \\ 0.318 & 0.178 & 0.622 & 0.532 & 0.022 \\ -0.354 & -0.205 & -0.175 & 0.022 & 0.837 \end{bmatrix}$$

- Test 3: The setting of Test 3 is the same as Test 2 with a different realization of  $A$ :

$$A = \begin{bmatrix} 1.340 & -0.824 & -0.078 & 0.325 & -0.840 \\ -0.824 & 1.161 & 0.098 & -0.543 & 0.402 \\ -0.078 & 0.098 & 0.868 & -0.389 & -0.473 \\ 0.325 & -0.543 & -0.389 & 0.747 & 0.222 \\ -0.840 & 0.402 & -0.473 & 0.222 & 1.339 \end{bmatrix}$$

In our numerical tables, “T1”, “T2” and “T3” refer to the Test 1, Test 2 and Test 3 defined above, respectively.

We compute the value function in the box  $[-1, 1]^d$ . So the initial values of the characteristics  $X_0^{(n)}$  are uniformly sampled from this box. But the characteristics are computed in the whole

space with sufficiently long time until  $e^{-\rho t}\Phi(X(t))$  and  $e^{-\rho t}\lambda(X(t))$  are both sufficiently small. Only the labelled data on the trajectories inside the box are used to train the model  $\hat{\Phi}_Q$ . The training process to minimize the loss  $L(\theta)$  uses the full-batch ADAM.

We measure the accuracy of the numerical solution  $\hat{\Phi}_Q$  by the average residual of HJB equation of  $N_p = 10000$  points uniformly selected from  $[-1, 1]^d$ :

$$\begin{aligned} error = \frac{1}{N_p} \sum_{j=1}^{N_p} & |\rho \hat{\Phi}_Q(x_j) - g(x_j, u^*(x_j)) \cdot \nabla \hat{\Phi}_Q(x_j) \\ & - l(x_j, u^*(x_j))| \end{aligned} \quad (5.35)$$

where  $u^*(x) = -B^\top \nabla \hat{\Phi}_Q(x)$ .

We design two experiments on each of the above three tests for different purposes to benchmark and understand our algorithms.

**Experiment 1.** In Experiment 1, we study how insufficient amount of characteristics data will affect the accuracy. Specifically, we change the number of the characteristic trajectories  $N$  between 2 and 10 while keep all other settings the same. Less trajectories means less amount of labelled data from the method of characteristics. At each policy iteration, the training for the supervised learning to minimize the loss  $L(\theta)$  takes a fixed number of 1000 ADAM steps or reaches a prescribed low tolerance. The number of policy iterations is fixed as 30.

Table I shows the results when  $\mu$  varies for each test. For each given  $N$ , the collection of  $N$  initial states are the same at different  $\mu$  for consistent comparison. If the numerical value of  $\Phi$  goes to infinity, we mark ‘‘Diverge’’ in the table. Otherwise the average residual-errors defined in (5.35) of the last 20 iterations is reported. For each setting, the best residual is highlighted in bold symbols and the worst residual (including the diverge case) is emphasised in italics. From Table I, we can see for all three tests,  $\mu = 1$  (only using the value ) or  $\mu = 0$  (only use the gradient-value) has the worst performance and may diverge in many cases, while the combination loss corresponding to  $\mu$  strictly between 0 and 1 can achieve the best accuracy and we do not see divergence at all. However, the value  $\mu$  corresponding to the best accuracy result changes from test to test. This table also confirms that with the increasing number  $N$  of characteristics, the final accuracy of the numerical value functions always gets better and better since more labelled data are provided.

To investigate the effect of  $\mu$  to the decay of the error, we plot the residual error of (5.35) during the policy iteration in Fig. 2. This figure clearly demonstrates that  $\mu = 1$  has the slowest

|     | $\mu$ | The number of characteristics trajectories $N$ |                |                |                |               |
|-----|-------|--|----------------|----------------|----------------|---------------|
|     |       | 2  | 4              | 6              | 8              | 10            |
| T1  | 1.0   | <i>Diverge</i>                                 | <i>Diverge</i> | <i>Diverge</i> | 0.0251         | 0.0080        |
|     | 0.8   | 0.0382   | 0.0069         | 0.0032         | 0.0027         | 0.0024        |
|     | 0.6   | 0.0251   | 0.0056         | 0.0022         | 0.0018         | 0.0016        |
|     | 0.4   | <b>0.0088</b>                                  | 0.0041         | 0.0020         | 0.0016         | 0.0019        |
|     | 0.2   | 0.0017   | 0.0030         | <b>0.0015</b>  | 0.0019         | 0.0014        |
|     | 0.0   | 0.0106   | <b>0.0026</b>  | 0.0022         | <b>0.0013</b>  | <b>0.0012</b> |
|     | T2    | 1.0  | 2.9116         | <i>Diverge</i> | 0.0860         | 0.0281        |
| 0.8 |       | 0.0360   | <b>0.0097</b>  | 0.0049         | 0.0060         | 0.0058        |
| 0.6 |       | 0.0370   | 0.0128         | <b>0.0046</b>  | 0.0058         | <b>0.0045</b> |
| 0.4 |       | <b>0.0193</b>                                  | 0.0204         | 0.0140         | <b>0.0044</b>  | 0.0057        |
| 0.2 |       | 0.0280   | 0.0193         | 0.0220         | 0.0198         | 0.0094        |
| 0.0 |       | <i>Diverge</i>                                 | <i>Diverge</i> | 0.0358         | 0.0085         | 0.0413        |
| T3  |       | 1.0  | 6.3956         | 1.3894         | 0.1372         | 0.0262        |
|     | 0.8   | <b>0.0544</b>                                  | <b>0.0269</b>  | 0.0259         | <b>0.0153</b>  | 0.0120        |
|     | 0.6   | 0.1079   | 0.0365         | <b>0.0236</b>  | 0.0162         | <b>0.0081</b> |
|     | 0.4   | 0.0806   | 0.0833         | 2.6797         | 0.1816         | 0.0203        |
|     | 0.2   | <i>Diverge</i>                                 | 0.0754         | 0.2794         | 31.3591        | 0.0481        |
|     | 0.0   | <i>Diverge</i>                                 | 0.1773         | <i>Diverge</i> | <i>Diverge</i> | 0.0834        |

TABLE I: Error (HJB residual) for various  $\mu$  when the number of trajectories  $N$  changes. “T1”, “T2” and “T3” refer to the three tests in the text.

convergence among all  $\mu$  we tested, and we can find that adding even a small portion of the loss for the value-gradient, i.e.,  $\mu < 1$ , can improve the convergence.

**Experiment 2.** The purpose of Experiment 2 is to test the performance of the methods when the training process is not exact. Recall that in Experiment 1, we have set the maximum steps in training process as a sufficiently large number 1000. Here, we limit this maximum training step to the range  $10 \sim 200$ . A small maximum training step means less accuracy in fitting the value function. For each test, the algorithm is run up to 120 policy iterations and the number of characteristics trajectories is fixed as a relative small number  $N = 5$  now.

The average HJB residuals of the last 20 policy iterations are reported in Table II to measure the accuracy. This table shows that  $\mu = 1$  has the worst performance in Test 1 and Test 2 and neither  $\mu = 1$  or  $\mu = 0$  can perform well in Test 3. It is confirmed that the setting of  $\mu$  strictly between 0 and 1 is more robust to incomplete training and also has better performance in accuracy. We can also see from this table that there is in general no necessity to use a strict stopping criteria for training the interpolation for  $\hat{\Phi}_Q$ . Even a small training step 10 with a choice

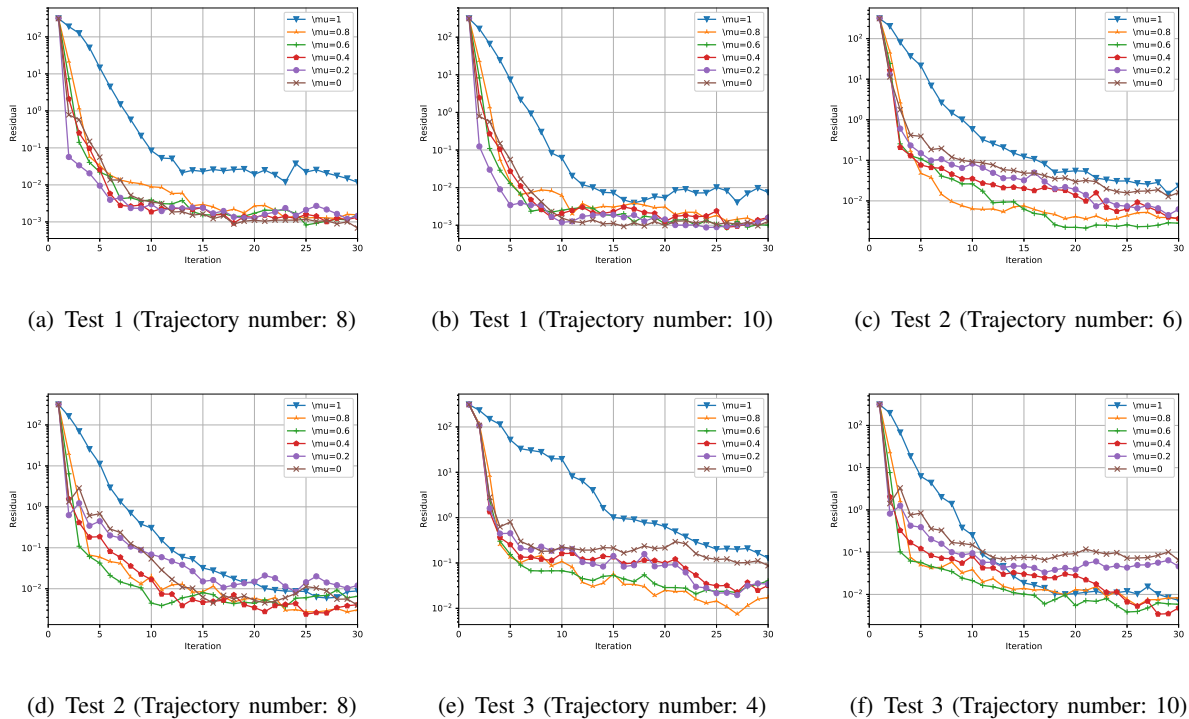


Fig. 2: Error (HJB residual) vs policy iteration for various  $\mu$ .

|    | $\mu$ | Train step     |                |                |                |                |
|----|-------|----------------|----------------|----------------|----------------|----------------|
|    |       | 10             | 50             | 100            | 150            | 200            |
| T1 | 1.0   | 1.476          | Diverge        | Diverge        | 1.03e-2        | 1.55e-2        |
|    | 0.8   | <b>4.36e-4</b> | <b>4.46e-4</b> | <b>4.58e-4</b> | <b>4.57e-4</b> | <b>4.51e-4</b> |
|    | 0.6   | 6.12e-4        | 6.18e-4        | 6.25e-4        | 6.25e-4        | 6.45e-4        |
|    | 0.4   | 7.02e-4        | 7.10e-4        | 7.14e-4        | 7.12e-4        | 7.30e-4        |
|    | 0.2   | 7.62e-4        | 7.66e-4        | 7.68e-4        | 7.70e-4        | 7.84e-4        |
|    | 0.0   | 8.04e-4        | 8.02e-4        | 8.08e-4        | 8.10e-4        | 8.19e-4        |
| T2 | 1.0   | 0.146          | Diverge        | Diverge        | Diverge        | Diverge        |
|    | 0.8   | <b>2.93e-4</b> | <b>2.80e-4</b> | <b>2.84e-4</b> | <b>2.88e-4</b> | <b>2.92e-4</b> |
|    | 0.6   | 4.13e-4        | 3.88e-4        | 3.83e-4        | 3.83e-4        | 3.82e-4        |
|    | 0.4   | 4.42e-4        | 4.51e-4        | 4.46e-4        | 4.46e-4        | 4.36e-4        |
|    | 0.2   | 4.56e-4        | 4.87e-4        | 4.57e-4        | 4.70e-4        | 4.76e-4        |
|    | 0.0   | 4.83e-4        | 5.15e-4        | 4.98e-4        | 5.07e-4        | 2.23e-3        |
| T3 | 1.0   | 7.47e-2        | Diverge        | 5.91e-4        | 8.48e-4        | 1.21e-2        |
|    | 0.8   | 3.53e-4        | <b>2.32e-4</b> | <b>2.36e-4</b> | 2.45e-4        | <b>2.61e-4</b> |
|    | 0.6   | <b>3.39e-4</b> | 3.06e-4        | 3.17e-4        | 3.35e-4        | 3.19e-4        |
|    | 0.4   | 4.31e-4        | 3.59e-4        | 3.56e-4        | 3.65e-4        | 7.77e-4        |
|    | 0.2   | 4.53e-4        | 3.96e-4        | 4.07e-4        | <b>1.08e-4</b> | 1.05e-2        |
|    | 0.0   | 5.09e-4        | 4.20e-4        | 8.48e-3        | 5.20e-3        | 8.31e-3        |

TABLE II: Error (HJB residual) for various  $\mu$  when the training steps change.

$\mu \in (0, 1)$  can have the same final accuracy as the large training step 200.

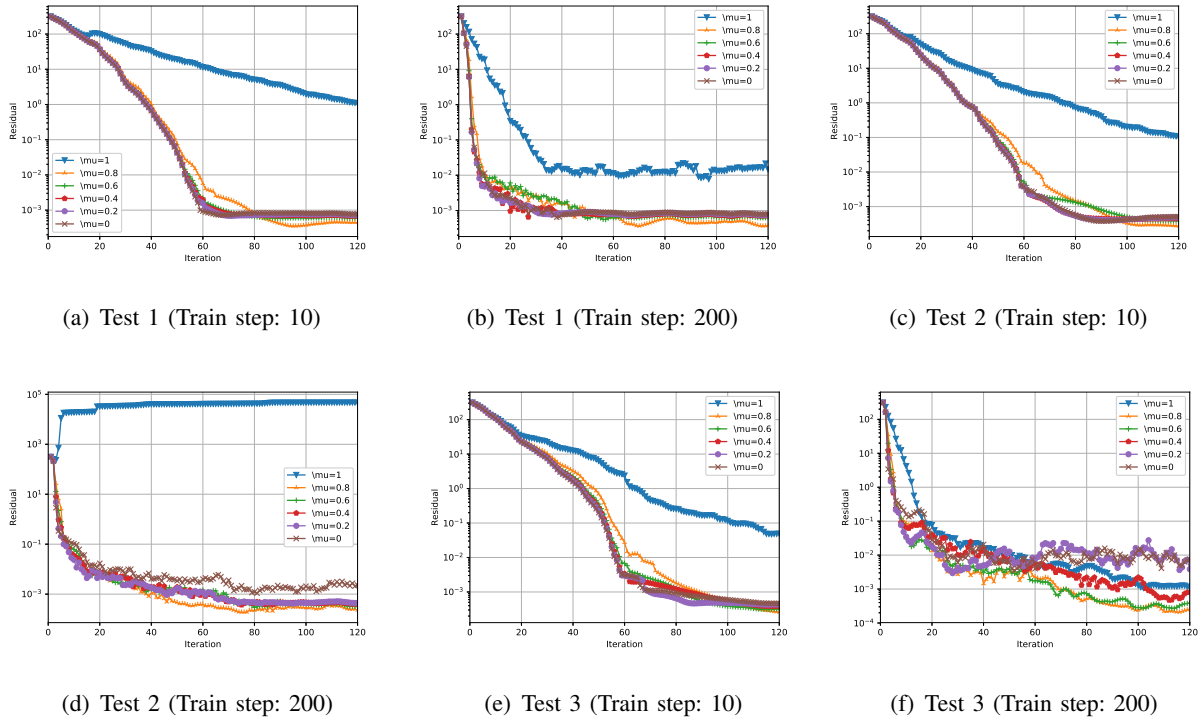


Fig. 3: Error (HJB residual) vs policy iteration for various  $\mu$ . The trajectory number is 5.

Fig. 3 shows the convergence of the policy iteration at different  $\mu$  values. We see that again for all three tests,  $\mu = 1$  corresponding to the policy iteration with only the value function, gives the slowest decay of error among all  $\mu$  tests. For other values of  $\mu < 1$ , the performances of reducing the error are basically similar and all outperform the case of  $\mu = 1$ .

In summary, for the toy model of linear-quadratic problem, we have conducted many numerical tests to show the advantage of our formulation of using the value-gradient data in training the value function: it improves the convergence of the policy iteration and shows much better robustness for a limited amount of data and a limited number of training steps. The performance comparisons for the general nonlinear problems are presented in the next for two other examples.

### B. Pendulum swing-up task

The second example is a 2-dim nonlinear case, the pendulum swing-up task [16] (see Fig. 4). The physical model includes a pole and a ball. One end of the pole is fixed to the wall so

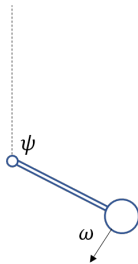


Fig. 4: Sketch map of pendulum swing-up task

that the pole can swing around it, the other end of the pole is connected to the ball. The aim of this task is to swing-up the ball and balance it in the vertical direction.

The state of this problem has two dimensions. The angular velocity of the ball, denoted by  $\omega$ ; the included angle of the pole and the vertical direction, denoted by  $\psi \in [-\pi, \pi]$ . If the pole is overturned,  $\psi$  will be modulated to the corresponding value between  $-\pi$  and  $\pi$ . The control of this problem is the moment applied to the ball, denoted by  $u$ . If the ball is successfully swung up and balanced at the vertical direction,  $\psi = 0$ . Thus we want the absolute value of  $\psi$  to be as small as possible, and equivalently, we aim at minimizing  $-\cos(\psi)$ . Then this problem can be written as a control problem with the cost function

$$J(u) = \int_0^{\infty} -e^{-\rho t} \cos(\psi) dt$$

subject to the dynamic system

$$\begin{cases} \frac{d\omega}{dt} = \frac{1}{ml^2}(-\gamma\omega + mgl \sin(\psi) + u), \\ \frac{d\psi}{dt} = \omega, \quad \mu(0) = \mu_0, \psi(0) = \psi_0 \end{cases}$$

where  $m$  is the mass of the ball,  $l$  is the length of the pole,  $g$  is the gravitational constant. And a constraint is imposed on the control:  $|u| \leq u_{max}$ . Here  $u_{max} \geq 0$  is the largest control we can have. These hyper-parameters are set to be

$$\rho = 5, m = 1, l = 1, \gamma = 0.01, u_{max} = 5.$$

The value function is parametrized as a family of radial basis functions as follows

$$\widehat{\Phi}(\mathbf{x}; w, s, c) = \sum_{i=1}^n w_i e^{-\|s_i^T(\mathbf{x}-c_i)\|^2} \quad (5.36)$$

where  $\mathbf{x} = (\omega, \psi)$  is the state variable and  $w_i \in \mathbb{R}, \mathbf{s}_i, \mathbf{c}_i \in \mathbb{R}^d$  are the set of parameters  $\theta$ . The number of modes  $n$  is chosen to be 25, so there are totally  $(2d+1)n = 125$  parameters to learn. We compute the value function on the domain  $[-2\pi, 2\pi) \times [-\pi, \pi) \subset \mathbb{R} \times [-\pi, \pi)$ .

The accuracy of the numerical value function is also measured by the residual of the HJB equation like (5.35) based on  $N_p = 100$  grid-points in  $[-2\pi, 2\pi) \times [-\pi, \pi)$ . One remark is that at  $\mu = 0$ , we only use the value-gradient data and can only find the gradient of the value function. So there is an additive constant in the value function  $\widehat{\Phi} + const$  to be further determined. We practically use the least square fitting to determine this constant based on the HJB equation.

Another important indicator to measure the performance for our pendulum swing-up problem is the so-called ‘‘successful roll-up numbers’’. For a given initial state  $(\omega(0), \psi(0))$ , the trajectory  $\psi(t)$  is simulated with the given policy up to time  $T$ . If the maximum time duration  $t_2 - t_1$  whenever  $|\psi(t)| < \pi/4$  for  $t \in (t_1, t_2)$ , exceeds a threshold  $\tau$ , it is called a ‘‘successful roll-up’’. For a given policy, we first uniformly select the 100 pairs of  $(\omega(0), \psi(0))$  from  $[-2\pi, 2\pi) \times [-\pi, \pi)$  as the initial states and set the total simulation time  $T = 20$  and the roll-up threshold time duration  $\tau = 10$ . So a larger number of ‘‘successful roll-up’’ means the current policy can better stabilize the pendulum toward the vertical position.

|                     | $\mu$ | Number of trajectories |              |              |
|---------------------|-------|------------------------|--------------|--------------|
|                     |       | 2                      | 5            | 10           |
| Residual            | 1.0   | <i>1.532</i>           | <i>1.060</i> | <i>0.586</i> |
|                     | 0.8   | 0.581                  | 0.246        | <b>0.102</b> |
|                     | 0.6   | 0.510                  | <b>0.077</b> | 0.126        |
|                     | 0.4   | 0.299                  | 0.224        | 0.227        |
|                     | 0.2   | 0.345                  | 0.211        | 0.098        |
|                     | 0.0   | <b>0.246</b>           | 0.081        | 0.122        |
| Successful roll-ups | 1.0   | 5.40                   | 2.20         | 1.60         |
|                     | 0.8   | 2.55                   | 3.80         | <b>82.95</b> |
|                     | 0.6   | 21.15                  | <b>75.20</b> | 53.60        |
|                     | 0.4   | 16.45                  | 36.10        | 30.25        |
|                     | 0.2   | 16.05                  | 31.65        | 75.80        |
|                     | 0.0   | <b>36.65</b>           | 65.30        | 26.35        |

TABLE III: The HJB residual and successful roll-up numbers in pendulum swing-up task. The smaller residual and the larger successful roll-up number are better results. The best value of  $\mu$  are highlighted in bold symbols and the worst value are marked in italics. The train step is 50.

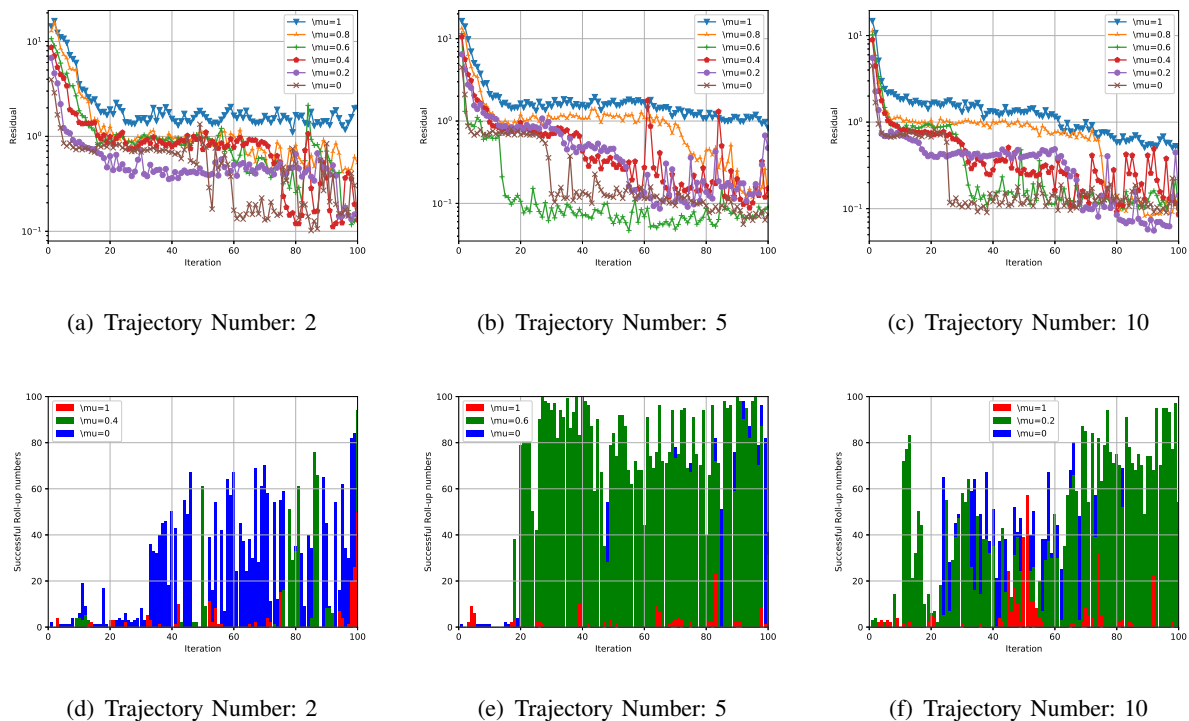


Fig. 5: Residual and successful roll-up numbers during the 100 policy iteration for various  $\mu$  in the pendulum swing-up task.

|                     | $\mu$ | Train step   |              |              |              |
|---------------------|-------|--------------|--------------|--------------|--------------|
|                     |       | 25           | 50           | 75           | 100          |
| Residual            | 1.0   | 0.170        | 0.586        | 0.208        | 0.353        |
|                     | 0.8   | 0.148        | 0.102        | 0.297        | 0.168        |
|                     | 0.6   | <b>0.119</b> | 0.126        | 0.101        | 0.216        |
|                     | 0.4   | 0.120        | 0.227        | 0.123        | 0.141        |
|                     | 0.2   | 0.458        | <b>0.098</b> | 0.098        | 0.065        |
|                     | 0.0   | 0.127        | 0.122        | <b>0.070</b> | <b>0.062</b> |
| Successful roll-ups | 1.0   | 12.55        | 1.60         | 6.10         | 43.75        |
|                     | 0.8   | 23.80        | <b>82.95</b> | 33.35        | 50.50        |
|                     | 0.6   | <b>58.30</b> | 53.60        | 66.30        | 42.00        |
|                     | 0.4   | 26.25        | 30.25        | 41.20        | 55.90        |
|                     | 0.2   | 15.80        | 75.80        | 48.95        | 65.25        |
|                     | 0.0   | 56.50        | 26.35        | <b>77.80</b> | <b>81.10</b> |

TABLE IV: The residual and successful roll-up numbers for various  $\mu$  when training steps varies in the pendulum swing-up task. The trajectory number is 10.



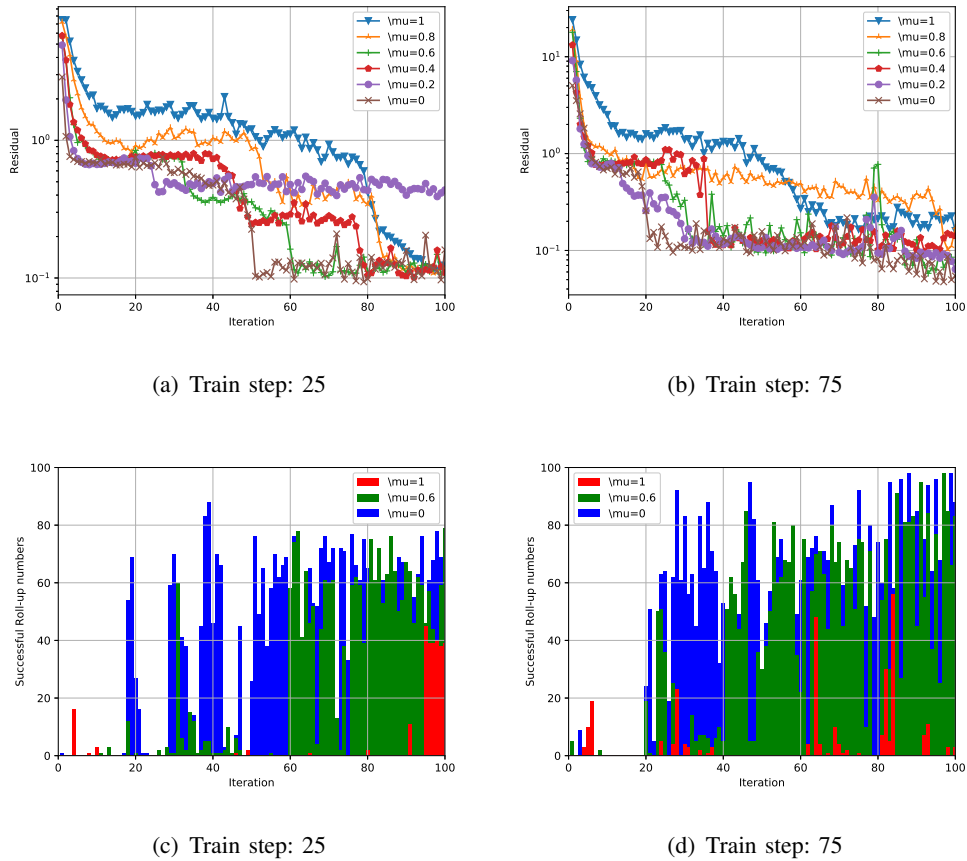


Fig. 6: Residual and successful roll-up numbers during the policy iteration with training steps of 25 and 75 in pendulum swing-up task.

Likely to the previous linear-quadratic example, we also conduct two experiments to test the performance of the methods. The total number of policy iteration is 120.

**Experiment 1.** In Experiment 1, the trajectory number of 2, 5 and 10 are tested. Table III records the average error and average successful roll-up numbers of the last 20 iterations after the total 120 policy iterations. As shown in Table III,  $\mu = 1$  has the worst accuracy and the extremely poor number of successful roll-ups. Fig. 5 shows the residual and successful roll-up numbers with respect to the policy iteration number. In particularly, in the second row of Fig. 5 we compute the successful roll-up numbers during the policy iteration by independently simulating the dynamics with the current control. This figure demonstrates that the value-gradient formulation has the phenomenal performance to boost the successful roll-ups.

**Experiment 2.** In Experiment 2, we test the train step and Table IV records the residual errors

and successful roll-up numbers as before for train steps taking values 25, 50, 75 and 100. Fig. 6 plots the decay of the errors and the progress of the successful roll-ups. Like Experiment 1, we have the same conclusion that across different trajectory numbers  $N$ , the mixture of the value and its gradient with  $\mu \in (0, 1)$  are much better than the formulation of only value function

### C. Cart-pole balancing task

The last example is the 4-dim nonlinear case of the cart-pole balancing task [2] (see Fig. 7). The physical model of this task includes a car, a pole and a ball. The ball is connected to one

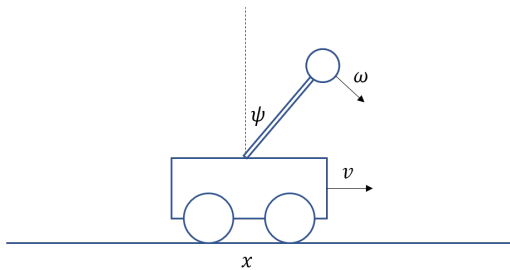


Fig. 7: Sketch map of cart-pole balancing task

end of the pole and the other end of the pole is fixed to the car. The pole can rotate around the end fixed to the car, while the car is put on a flat surface, being able to move left or right. The aim of this task is to balance the pole in the upright vertical direction.

The state variable has four dimensions. The angular velocity of the ball, denoted by  $\omega$ ; the included angle of the pole and the vertical direction, denoted by  $\psi \in [-\pi, \pi]$ ; the velocity of the car, denoted by  $v$ ; the position of the car, denoted by  $x$ . The control of this problem is the force applied to the car, denoted by  $F$ .

The control problem is to let  $\psi$  be as small as possible. To eliminate the translation invariant in the horizontal position  $x$ , we also want  $x$  to be small. So we aim to minimize  $-\cos(\psi)$  and  $\|x\|^2$  with the following cost function

$$J(u) = \int_0^{\infty} e^{-\rho t} (-\cos(\psi) + \eta \|x\|^2) dt$$

with  $\rho = 5$  and  $\eta = 0.2$  and subject to the dynamic system

$$\begin{cases} \dot{\omega} = \frac{g \sin \psi + \frac{(\mu_c \operatorname{sgn}(v) - F - ml\omega^2 \sin \psi) \cos \psi}{m+m_c} - \frac{\mu_p \omega}{ml}}{l \left( \frac{4}{3} - \frac{m}{m+m_c} \cos^2 \psi \right)} \\ \dot{\psi} = \omega \\ \dot{v} = \frac{F + ml(\omega^2 \sin \psi - \dot{\omega} \cos \psi) - \mu_c \operatorname{sgn}(v)}{m + m_c} \\ \dot{x} = v \\ \omega(0) = \omega_0, \psi(0) = \psi_0, v(0) = v_0, x(0) = x_0 \end{cases}$$

where  $m$  is the mass of the ball,  $m_c$  is the mass of the car,  $l$  is the length of the pole,  $g$  is the gravitational constant. A constraint is imposed to the control:  $|F| \leq F_{max}$ ,  $F_{max} \geq 0$  is the largest control we can have. These hyper-parameters are set to be

$$\begin{aligned} m &= 0.1, l = 0.5, m_c = 1, \mu_c = 0.0005, \\ \mu_p &= 0.000002, F_{max} = 10, \end{aligned}$$

The state variable is  $\mathbf{x} = (\omega, \psi, v, x) \in \mathbb{R}^4$  with  $\psi \in [-\pi, \pi]$  as in the pendulum example. The value function is approximated by the radial function as in (5.36): with  $n = 50$  modes. Totally, there are  $(2d + 1)n = 450$  parameters to learn. We compute the value function on the domain  $\Omega = [-2\pi, 2\pi] \times [-\pi, \pi] \times [-0.5, 0.5] \times [-2.4, 2.4]$ .

The error is also measured by the HJB residual as in (5.35) calculated on 10000 points uniformly sampled from  $\Omega$ . We also define the successful roll-up, if  $|\psi(t)| < \pi/4$  lasts for 10 seconds and  $|x(t)| < 10$  for all  $t \in [0, T]$  where we simulate the dynamics up to time  $T = 20$  seconds. The initial condition for measuring the successful roll-up numbers are  $(\omega(0), \psi(0), v(0) = 0, x(0) = 0)$  with 100 pairs of  $(\omega(0), \psi(0))$  from the  $10 \times 10$  mesh grid of  $[-2\pi, 2\pi] \times [-\pi, \pi]$ .

We also conduct the two experiments for this 4-dim nonlinear case to test the performance with insufficient data or incomplete training. The total number of policy iteration is fixed as 50.

**Experiment 1.** In Experiment 1, three trajectory numbers of 2, 5 and 10 are tested with 100 train steps at each policy iteration. **Experiment 2.** In Experiment 2, the train steps 50, 100, 150 and 200 are tested. The trajectory number is now fixed as 10. As shown in Table V and Table VI, the accuracy gets quite remarkable improvements as long as the value-gradient is included in the formulation. The successful roll-ups also show a better performance for  $\mu < 1$ , particularly when the number of trajectories increases. Fig. 8 and Fig. 9 show the residual and successful

|                       | $\mu$ | Number of trajectories |              |              |
|-----------------------|-------|------------------------|--------------|--------------|
|                       |       | 2                      | 5            | 10           |
| Residual              | 1.0   | 2.088                  | 0.844        | 0.934        |
|                       | 0.8   | 0.696                  | 0.281        | 0.100        |
|                       | 0.6   | 0.450                  | 0.169        | 0.117        |
|                       | 0.4   | 0.441                  | 0.147        | 0.091        |
|                       | 0.2   | 0.181                  | <b>0.113</b> | <b>0.082</b> |
|                       | 0.0   | <b>0.166</b>           | 0.124        | 0.094        |
| Successful<br>roll-up | 1.0   | 14.85                  | 19.25        | 12.30        |
|                       | 0.8   | 10.65                  | 25.10        | <b>60.8</b>  |
|                       | 0.6   | <b>27.10</b>           | 25.15        | 38.65        |
|                       | 0.4   | 11.05                  | 39.25        | 44.20        |
|                       | 0.2   | 9.3                    | 40.95        | 50.45        |
|                       | 0.0   | 20.95                  | <b>44.95</b> | 55.00        |

TABLE V: The error (HJB residual) and the number of successful roll-ups for different  $\mu$  when the trajectory number  $N$  changes in the cart-pole balancing task. The train step is 100.

roll-ups with respect to the policy iteration for both experiments. As expected, choosing  $\mu < 1$  gets these results considerably improved.

|                       | $\mu$ | Train step   |              |              |              |
|-----------------------|-------|--------------|--------------|--------------|--------------|
|                       |       | 50           | 100          | 150          | 200          |
| Residual              | 1.0   | 1.355        | 0.934        | 0.500        | 0.471        |
|                       | 0.8   | 0.260        | 0.100        | 0.151        | 0.155        |
|                       | 0.6   | 0.175        | 0.117        | <b>0.092</b> | 0.097        |
|                       | 0.4   | <b>0.096</b> | 0.091        | 0.105        | 0.103        |
|                       | 0.2   | 0.106        | <b>0.082</b> | 0.094        | <b>0.080</b> |
|                       | 0.0   | 0.130        | 0.094        | 0.070        | 0.083        |
| Successful<br>roll-up | 1.0   | 13.75        | 12.30        | 28.55        | 30.00        |
|                       | 0.8   | 58.25        | <b>60.80</b> | 41.45        | 35.80        |
|                       | 0.6   | 28.05        | 38.65        | 16.50        | 35.55        |
|                       | 0.4   | 56.40        | 44.20        | 36.50        | 35.75        |
|                       | 0.2   | <b>61.65</b> | 50.45        | 35.30        | 47.00        |
|                       | 0.0   | 21.85        | 55.00        | <b>49.30</b> | <b>54.10</b> |

TABLE VI: The error (HJB residual) and the number of successful roll-ups for different  $\mu$  when training steps change in the cart-pole balancing task. The trajectory number is 10.

To conclude the above three examples, we have performed the numerical tests by changing the amount of characteristics data and the training steps, which are two important factors in practical computation. By comparing the performance measured by the HJB residual as the error and the

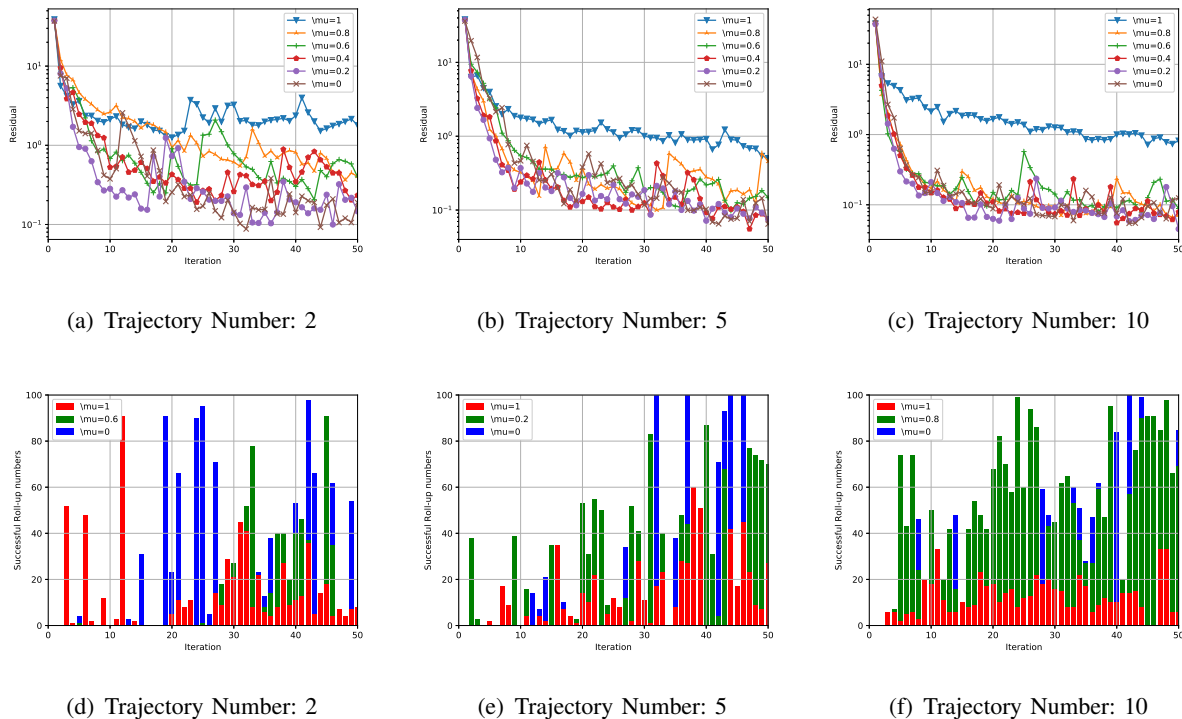


Fig. 8: Residual and the successful roll-ups with trajectory number of 2, 5 and 10 in the cart-pole task. The train step is 100.

successful roll-ups as the robustness, we find that these numerical results consistently show the outperformance when using the characteristics data both from the value and the value-gradient functions. Although the four tested values of  $\mu = 0.2, 0.4, 0.6, 0.8$  between 0 and 1 always beat the traditional method at  $\mu = 1$ , the optimal value  $\mu$  actually varies on the specific settings and the difference among these four values for the performance is marginal.

## VI. CONCLUSION

Based on the system of PDEs for the value-gradient functions we derived in this paper and the traditional HJB equation for the value function, we develop a new policy iteration framework, called **PI-lambda**, for the numerical solution of the value function for the optimal control problems. The systems of PDEs for the value-gradient functions are essentially decoupled and shares the same characteristics ODE with the generalized HJB equation. By simulating characteristics curves in parallel for the state variable by any classic ODE solver (like Runge-Kutta method), our method generates both the value  $\Phi$  and the value-gradient functions  $\nabla\Phi$

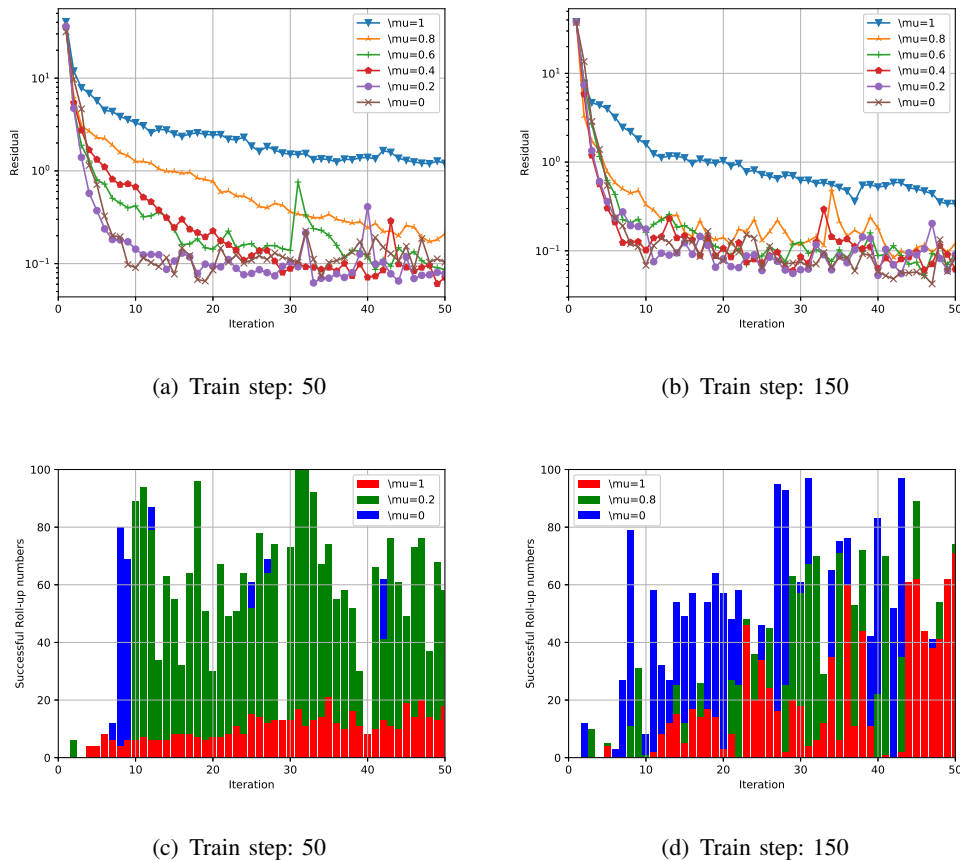


Fig. 9: Residual and successful roll-up number vs iteration values with training steps of 50 and 150 in the cart-pole task.

on each characteristics. Equipped with any state-of-the-art function representation techniques and the large-scale minimization techniques from supervised learning and deep learning, these labelled data can be generalized to the whole space to attack high dimensional problems. The utilization of policy iteration has the computational convenience to simulate the characteristics equations only forward in time so as to improve the policy gradually, instead of solving any boundary-value problem for *optimal* trajectories directly as in [22], [25], [28]. The learning procedure of supervised learning in our method is not new, and it has been applied, for example in [22], [29], [36], to learn the policy, the value function and the value-gradient function together if the corresponding datasets are available. Our major contribution is to formulate the co-state variable as the gradient function  $\lambda(x)$  of state, not a function of time  $\lambda(t)$  in PMP.

The generalization of our main theorem Theorem 2 to the finite horizon control problem

on  $[0, T]$  is straightforward: to replace  $\rho\lambda(x)$  by  $-\partial_t\lambda(t, x)$  in equation (3.21) and add the transversality condition  $\lambda(T, x) = \nabla_x h(T, x)$  when there is a terminal cost  $h(T, x(T))$ . The main algorithm in this paper based on the policy iteration, **PI-lambda**, illustrated in Figure 1 is still applicable and in such cases, one needs to parametrize the time-dependent function  $\lambda(t, x)$  with additional time variable  $t$ .

Some practical computational issues which are not fully discussed here include the choice of the initial policy  $a^0$ , the number of trajectories  $N$  and their initial locations  $\{X_0\}$ . For the initial policy, it should be chosen conservatively to stabilize the dynamics. For the characteristics curves,  $N$  may be changed from iteration to iteration, and adaptive sampling for the initial states is a good question for further exploration. If a neural network is used, the network structure is also an important practical issue [29]. These questions all belong to the common problems in implementation for the policy iteration and supervised learning.

An obvious question to address in future is how to formulate the equations of  $\lambda$  for the stochastic optimal control so as to leverage the similar benefit of our algorithm for the deterministic control problem.

#### ACKNOWLEDGMENT

Alain Bensoussan acknowledges the financial support from the National Science Foundation under grants DMS-1612880, DMS-1905449, and the Research Grant Council of Hong Kong Special Administrative Region under grant GRF 11303316. Phillip Yam acknowledges the financial supports from HKGRF-14300717 with the project title “*New kinds of Forward-backward Stochastic Systems with Applications*”, HKGRF-14300319 with the project title “*Shape-constrained Inference: Testing for Monotonicity*”, and Direct Grant for Research 2014/15 (Project No. 4053141) offered by CUHK. Xiang Zhou acknowledges the support of Hong Kong RGC GRF grants 11337216 and 11305318.

#### REFERENCES

- [1] Alessandro Alla, Maurizio Falcone, and Dante Kalise. An efficient policy iteration algorithm for dynamic programming equations. *SIAM Journal on Scientific Computing*, 37(1):A181–A200, 2015.
- [2] Sutton Barto. Neuronlike adaptive elements that can solve difficult learning control problems. *IEEE Transactions on Systems, Man, and Cybernetics*, 13:834–846, 1983.
- [3] Randal W. Bea. Successive Galerkin approximation algorithms for nonlinear optimal and robust control. *International Journal of Control*, 71(5):717–743, 1998.

- [4] R W Beard, G N Saridis, and J T Wen. Approximate solutions to the time-invariant Hamilton–Jacobi–Bellman equation. *Journal of Optimization Theory and Applications*, 96(3):589–626, 1998.
- [5] Randal W. Beard, George N. Saridis, and John T. Wen. Galerkin approximations of the generalized Hamilton-Jacobi-Bellman equation. *Automatica*, 33(12):2159–2177, 1997.
- [6] R Bellman. *Dynamic Programming*. Princeton University Press, 1957.
- [7] Richard Bellman. A Markovian Decision Process. *Indiana University Mathematics Journal*, 6(4):679–684, 1957.
- [8] A Bensoussan. *Estimation and Control of Dynamical Systems*. Interdisciplinary Applied Mathematics. Springer International Publishing, 2018.
- [9] Alain Bensoussan, Yiqun Li, Dinh Phan Cao Nguyen, Minh-Binh Tran, Sheung Chi Phillip Yam, and Xiang Zhou. Machine Learning and Control Theory. *arXiv e-prints*, page arXiv:2006.05604, June 2020.
- [10] D. P. Bertsekas. *Dynamic Programming and Optimal Control, Vol. I, 2nd Ed.* Athena Scientific, Belmont, MA, 2001.
- [11] D. P. Bertsekas. *Reinforcement Learning and Optimal Control*. Athena Scientific, Belmont, MA, 2019.
- [12] Yat Tin Chow, Jérôme Darbon, Stanley Osher, and Wotao Yin. Algorithm for overcoming the curse of dimensionality for time-dependent non-convex hamilton–jacobi equations arising from optimal control and differential games problems. *Journal of Scientific Computing*, 73(2):617–643, 2017.
- [13] Yat Tin Chow, Jérôme Darbon, Stanley Osher, and Wotao Yin. Algorithm for overcoming the curse of dimensionality for certain non-convex hamilton–jacobi equations, projections and differential games. *Annals of Mathematical Sciences and Applications*, 3(2):369–403, 2018.
- [14] Yat Tin Chow, Wuchen Li, Stanley Osher, and Wotao Yin. Algorithm for Hamilton–Jacobi equations in density space via a generalized Hopf formula. *Journal of Scientific Computing*, 80(2):1195–1239, 2019.
- [15] Jérôme Darbon and Stanley Osher. Algorithms for overcoming the curse of dimensionality for certain hamilton–jacobi equations arising in control theory and elsewhere. *Research in the Mathematical Sciences*, 3(1):1–26, 2016.
- [16] Kenji Doya. Reinforcement learning in continuous time and space. *Neural Computation*, 12(1):219–245, 2000.
- [17] Maurizio Falcone and Roberto Ferretti. *Semi-Lagrangian approximation schemes for linear and Hamilton–Jacobi equations*. SIAM, 2013.
- [18] W H Fleming and R W Rishel. *Deterministic and Stochastic Optimal Control*. Stochastic Modelling and Applied Probability. Springer New York, 1975.
- [19] W.H. Fleming and H.M. Soner. *Controlled Markov Processes and Viscosity Solutions*. Stochastic Modelling and Applied Probability. Springer New York, 2006.
- [20] M. B. Horowitz, A. Damle, and J. W. Burdick. Linear hamilton jacobi bellman equations in high dimensions. In *53rd IEEE Conference on Decision and Control*, pages 5880–5887, 2014.
- [21] Ronald A. Howard. *Dynamic programming and Markov processes*. The Technology Press of M.I.T., Cambridge, Mass.; John Wiley & Sons, Inc., New York-London, 1960.
- [22] Dario Izzo, Ekin Öztürk, and Marcus Märtens. Interplanetary transfers via deep representations of the optimal policy and/or of the value function. In *Proceedings of the Genetic and Evolutionary Computation Conference Companion, GECCO '19*, page 1971–1979, New York, NY, USA, 2019. Association for Computing Machinery.
- [23] Dante Kalise and Karl Kunisch. Polynomial approximation of high-dimensional Hamilton-Jacobi-Bellman equations and applications to feedback control of semilinear parabolic PDES. 40(2):629–652.
- [24] Wei Kang and Lucas Wilcox. A causality free computational method for HJB equations with application to rigid body satellites. In *AIAA Guidance, Navigation, and Control Conference*, page 2009, 2015.
- [25] Wei Kang and Lucas C. Wilcox. Mitigating the curse of dimensionality: sparse grid characteristics method for optimal feedback control and hjb equations. *Computational Optimization and Applications*, 68(2):289–315, 2017.



- [26] Diederik P Kingma and Jimmy Ba. Adam: A method for stochastic optimization. *arXiv preprint arXiv:1412.6980*, 2014.
- [27] Alex Tong Lin, Yat Tin Chow, and Stanley J. Osher. A splitting method for overcoming the curse of dimensionality in Hamilton–Jacobi equations arising from nonlinear optimal control and differential games with applications to trajectory generation. *Communications in Mathematical Sciences*, 16(7), 1 2018.
- [28] T. Nakamura-Zimmerer, Q. Gong, and W. Kang. Qrnet: Optimal regulator design with lqr-augmented neural networks. *IEEE Control Systems Letters*, 5(4):1303–1308, 2021.
- [29] Tenavi Nakamura-Zimmerer, Qi Gong, and Wei Kang. Adaptive Deep Learning for High-Dimensional Hamilton-Jacobi-Bellman Equations. *arXiv e-prints*, page arXiv:1907.05317, July 2019.
- [30] Stanley Osher and James A Sethian. Fronts propagating with curvature-dependent speed: Algorithms based on hamilton-jacobi formulations. *Journal of Computational Physics*, 79(1):12–49, 1988.
- [31] Mathias Oster, Leon Sallandt, and Reinhold Schneider. Approximating the stationary Hamilton-Jacobi-Bellman equation by hierarchical tensor products. nov 2019.
- [32] L. S. Pontryagin. *Mathematical Theory of Optimal Processes*. CRC Press, 1987.
- [33] Martin L. Puterman and Shelby L. Brumelle. On the convergence of policy iteration in stationary dynamic programming. *Mathematics of Operations Research*, 4(1):60–69, 1979.
- [34] Benjamin Recht. A Tour of Reinforcement Learning: The View from Continuous Control. *Annual Review of Control, Robotics, and Autonomous Systems*, 2(1):253–279, 2019.
- [35] R S Sutton and A G Barto. *Reinforcement Learning: An Introduction*. Adaptive Computation and Machine Learning series. MIT Press, 2018.
- [36] Dharmesh Tailor and Dario Izzo. Learning the optimal state-feedback via supervised imitation learning. *Astrodynamics*, 3(4):361–374, 2019.
- [37] Yen-Hsi Richard Tsai, Li-Tien Cheng, Stanley Osher, and Hong-Kai Zhao. Fast sweeping algorithms for a class of Hamilton–Jacobi equations. *SIAM Journal on Numerical Analysis*, 41(2):673–694, 2003.
- [38] J. N. Tsitsiklis. Efficient algorithms for globally optimal trajectories. In *Proceedings of 1994 33rd IEEE Conference on Decision and Control*, volume 2, pages 1368–1373 vol.2, 1994.